International Geotechnical Symposium on Theory and Practice of Earth Reinforcement / Fukuoka Japan / 5-7 October 1988
 ISBN 906191 820 0

A review of field measurements of the behaviour of geogrid reinforced slopes and walls

Pietro Rimoldi
RDB Plastotecnica, Vigano, Italy

ABSTRACT: The paper present a review of papers dealing with field measurements for geogrid reinforced walls and slopes. Some comparisons and hypothesis are presented, in order to explain the field tests results. A proposal for the future research ends the paper.

1 INTRODUCTION

For some products used for earth reinforcement there are a good number of field and laboratory data currently available, particularly for steel bars and geotextiles. Instead, geogrids are currently well characterized by means of many laboratory tests which make the design engineers confident with the product, but both engineers and researchers are not confident with the mechanism of interaction between geogrids and soil structures, mainly because there are few field data from instrumented sections which can support design hypothesis. With the published papers on field measurements for geogrid reinforced soil, it is not possible to draw final conclusions but only to do some considerations to help the ongoing research. This is the aim of this paper.

2 DESIGN METHODS

The two design methods currently more widely used for geogrid reinforced soil projects are: the two-part wedge method for steep slopes (Jewell et al 1984), and the tie-back wedge method for vertical walls (Jones 1985). The method of Jewell for steep slopes is based on design charts which allow to obtain the coefficient of earth lateral pressure K^* and the reinforcement length L, as a function of the slope angle β and the angle of internal friction Φ', for a given value of the pore pressure ratio Ru. The charts were obtained from an extensive computer calculation of limit equilibrium based on two-part wedge failure mechanism. It assumes that the foundation is stable and the cohesion of the fill soil is equal to zero. The tie-back wedge method assumes a kinematic mechanism for wall movement of outward rotation around the toe; consequently it assumes that the active earth pressure is mobilized along the Rankine theoretical failure surface. The earth pressure is assumed to be resisted by the tensile forces developed in the geogrid layers, neglecting the resistance given by the wall face. In both methods the direct sliding on geogrids and the pull-out resistance are considered for the design of the length of reinforcement, based on a vertical pressure distribution assumed to be uniform of Meyerhof type.

3 CHECKING THE DESIGN

In order to check the currently available design methods or in order to develope new and more accurate design methods, the following data are needed:
- the distribution of σ_v and σ_h in the reinforced soil mass: they are essential for the proper calculation of settlements, of forces and displacements induced by direct sliding and pull-out mechanisms, and of the thrust to be resisted by the reinforcement;
- mechanism of soil reinforcement: can the soil develop the active pressure? how is the relative influence of interlocking and tensile resistance of geogrids?
- kinematic mechanism: in which cases it can be assumed to be a rotation around the toe or a two-part wedge rigid movement;
- distribution of tensile force along each geogrid layer: it will allow a correct evaluation of geogrid elongation and the comparison with the allowable tensile strength;
- diagram of geogrid strain versus time: these data will allow to know the in-soil

Table 1. List of the considered field tests.

No.	Location	Reference	Type	Description
1	Kagoshima (Japan)	Yamanouchi et al 1986	Wrap-around slope	78° slope, 6 m high, well graded volcanic sand, geogrid wrapped around sand bags at face;
2	Tucson (Arizona)	Berg et al 1986	full height panels concrete face wall	vertical wall, 1 ÷ 6 m high, sand soil, full height precast concrete facing panels;
3	Lithonia (Georgia)	Berg et al 1986	concrete face incremental wall	vertical wall, 6 m high, gravel soil, cruciform precast concrete facing panels;
4	Stanstead Abbotts (U.K.)	Bassett et al 1986	embankment on weak soil	embankment on peat soil, with one geogrid at base to distribute the load;
5	Gaspe Peninsula (Canada)	Berg et al 1987	concrete face incremental seawall	vertical wall for wave protection, 5.3 m high, sand-gravel soil, concrete panels of different shapes;
6	Cascade Dam (Michigan)	Christopher 1987	wrap-around vertical wall	retaining wall supporting a heavy weight crane, 3 m high, sand-gravel soil, wrap-around geogrids
7	Kingston (Canada)	Bathurst et al 1987	full height panels timber face wall	large scale laboratory test, 3 m high, sand soil, variable surcharge, full height timber panels;
8	Kingston (Canada)	Bathurst et al 1987	timber face incremental wall	large scale laboratory test, 3 m high, sand soil, variable surcharge, square timber panels;
9	Modena (Italy)	Cazzuffi et al 1988	steep sides embankment	embankment with 45° ÷ 60° side slopes, clay soil, wrap-around geogrids.

Table 2. Instruments used in the field tests

No. Location	Horizontal movement of face	Internal horizontal movements	Foundation settlements	Total stresses σ_h	σ_v	Pore pressure	Strains in geogrids	Forces in geogrids
1 Kagoshima	Survey reference points	-	-	-	-	-	strain gauges	-
2 Tucson	Survey reference points	-	-	load cells at face	load cells at base	-	strain gauges, inductance coils	-
3 Lithonia	Survey reference points	-	-	load cells at face	load cells at base	-	inductance coils	-
4 Stanstead	-	Horizontal profile gauge at base	Horizontal profile gauge, inclinometers	-	total pressure cells	p. p. gauges, pneum. piezom.	strain gauges, inductance coils	clamp load cells
5 Gaspe	Survey reference points	Multiple positions extensometer	-	total stress cells	-	pneum. piezom.	strain gauges	clamp load cells
6 Cascade	Survey reference points	wire extensometer	-	load cells at face	-	-	inductance and resistance strain g.	-
7 Kingston	electrical displacem. measuring device	-	-	-	earth press. cells at base	-	strain g. and tensioned steel wires	load cells at face
8 Kingston	electrical displacem. measuring device	-	-	-	earth press. cells at base	-	strain g. and tensioned steel wires.	load cells at face
9 Modena	-	-	settlements plates	-	-	-	strain gauges	clamp load cells

creep and consequently to fix a realistic limit to the tensile strength.
These data are needed for different types of load (uniform, linear, concentrated), for their practical range of values (for uniform surcharge it may be 0 ÷ 100 kPa).

4 FIELD TESTS AND INSTRUMENTATION USED

The field tests with published results are reported in Tab. 1: as it can be seen, two tests refer to steep slopes or embankments, one refers to an embankment on weak soil and six to vertical walls. The instruments used for each type of measurement in the considered field tests are described in Tab. 2. As it can be seen, in any case all the parameters were measured. Only in three cases both strains and tensile forces were recorded along some geogrid layers. The horizontal pressure was measured only at the face of the wall, but not in the soil mass and particularly not in the zone of maximum geogrid tensile forces. In each field test there were some interesting findings but, due to the little number of cases, they cannot be correlated in a general rule.

5 RESULTS

Tab. 3 shows a comparison of the results obtained in the considered field test; Stanstead Abbotts case was omitted in this list, since it is not really a slope reinforcement project but a base reinforcement one.
The values reported in Tab. 3 refer to three different conditions:
- Design condition (D): design values of parameters, used also to calculate strains ( ) and forces (α) in the geogrids;
- Calculation condition (C): real-situation-values of parameters, used also to calculate strains ( ) and forces (α) in the geogrids;
- Measured condition (M): the actual values.

In Tab. 3 the subscript D, C, M are used to indicate the above situations; symbols and formulas used are reported at the bottom.
In order to compare the results of the different field tests, some ratios, which can be regarded as partial Factors of Safety, were used; just from the analysis of Tab. 3, the following considerations can be drawn:
- the calculation with real-situation-values of parameters can give a gross estimate of actual forces and strains in the geogrids (FS1 = 1.0 ÷ 2.0), but if the soil is cohesive (Modena) they can be largely overestimated: this fact suggests that the mechanism of reinforcement for cohesive soils is slightly different from non-cohesive ones;
- a value of FSg of 1.1 ÷ 1.7 can lead to anticipate in the design far greater tensile forces than the actual ones (FS3 = 2.5 ÷ 10), and to a high ratio between allowable tensile strength and actual tensile forces (FS5 = 2.4 ÷ 13): this fact suggests that the actual design methods are conservative and can be used with a certain confidence;
- the previous consideration is not true if high line loads occur: in this case it's better to have more geogrid layers near the top than required from current design methods (Christopher 1987).

With a more accurate analysis of the published papers, all the cases can be reduced to three categories, based on the type of surcharge and of diagram of tensile forces:
Category 1) - slopes or embankment sides: as shown in Fig. 1, the tensile force has a smooth distribution along the geogrids; the maximum value is not at the base but in one of medium-low layers. If the slope angle β increases, the ratio $(x/H)_{max}$ decreases, in fact: $(x/H)_{max} \approx 0.30$ if $\beta = 45°$ (Modena); $(x/H)_{max} \approx 0.15$ if $\beta = 78°$ (Kagoshima). These results seem to be in agreement with the theory based on two-part wedge failure mechanism, but with cohesive soils the forces in the geogrids are lower than the calculated ones. If important settlements occur, then the tensile force in the base geogrid can arrive to relatively high values like 15 ÷ 20 kN/m (Bassett et al 1986).
Category 2) - vertical walls with uniformly distributed surcharge: as shown in Fig. 2 and Fig. 3, the tensile force diagram is different if the ratio $(q/\gamma H)$ is lower or greater of 0.8. In the former case there is a smooth pattern, with tensile forces increasing from top to bottom geogrid layer; the locus of maximum tensile force is a surface with an inclination $\Theta = (45° + \Phi'/2)$, coinciding with Rankine failure surface (Berg et al 1987). In the latter case, the tensile force diagram has a pronounced peak and the upper layers are more in tension than the lower ones; the locus of maximum tensile force is a surface close to the vertical ($\Theta = 0° \div 20°$), with $(x/H)_{max} \approx 0.15$. So, if the base can be considered not subjected to lateral movements and $(q/\gamma H) < 0.8$, then the failure mechanism is a rotation around the toe and the results seem in agreement with the tie-back wedge method. For higher values of the surcharge, the real mechanism needs to be further investigated.
Category 3) - vertical walls with high line loads: as shown in Fig. 4, the failure surface is approximately a logarithmic spiral, starting from the rear edge of the line load (Christopher 1987). The tensile forces are greater for the upper geogrid layers than for the lower ones, and for the upper layers forces can be greater than calculated with real-situation-values of parameters. With reference to the lateral pressure deve-

Table 3. Results of field tests

D = Design conditions; C = calculation conditions; M = measured conditions

No.	1			2			3			5			6			7			8			9		
Location	Kagoshima			Tucson			Lithonia			Gaspe			Cascade			Kingston			Kingston			Modena		
Geogrid used	Tensar SR2 (HDPE)			Tensar SR2 (HDPE)			Tensar SR2 (HDPE)			Tensar SR2 (HDPE)			Signode TNX250 (Polyester)			Tensar SR2 (HDPE)			Tensar SR2 (HDPE)			Tenax TT1 (HDPE)		
	D	C	M	D	C	M	D	C	M	D	C	M	D	C	M	D	C	M	D	C	M	D	C	M
H (m)	6.0	7.0	7.0	4.65	4.65	4.65	6.0	6.0	6.0	5.3	5.3	5.3	3.0	3.0	3.0	3.0	3.0	3.0	3.0	3.0	3.0	5.0	5.0	5.0
β (deg)	78	78	78	90	90	90	90	90	90	90	90	90	90	85	85	90	90	90	90	90	90	45	45	45
q (kPa)	9.8	0	0	12	12	?	12.9	12.9	?	37	37	37	80	80	80	12 50	12 50	12 50	12 50	12 50	12 50	10	0	0
γ (kN/m^3)	17.7	14.6	14.6	19.6	19.6	19.6	21.2	21.2	21.2	21.0	21.0	21.0	19.6	19.6	19.6	17.6	17.6	17.6	17.6	17.6	17.6	20.0	17.2	17.2
FSg (-)	1.70	1.0	1.0	1.11	1.0	1.0	1.16	1.0	1.0	1.16	1.0	1.0	1.30	1.0	1.0	?	1.0	1.0	?	1.0	1.0	1.10	1.0	1.0
Φ' (deg)	30	45	45	40	43	43	34	38	38	34	38	38	30	37	37	?	43	43	?	43	43	23	25	25
c' (kPa)	0	0	2.45	0	0	0	0	0	0	0	0	0	0	0	20	0	0	0	0	0	0	0	0	25
Ru (-)	0	0	0	0	0	0	0	0	0	0	0	0	0	0	0	0	0	0	0	0	0	0.25	0	0
α_f (kN/m)	78.5	-	-	80.0	-	-	80.0	-	-	80.0	-	-	50.0	-	-	80.0	-	-	80.0	-	-	66.0	-	-
α_a (kN/m)	31.4	-	-	29.0	-	-	29.0	-	-	21.5	-	-	(40)	-	-	29.0	-	-	29.0	-	-	30.0	-	-
N (-)	6	6	6	10	10	10	13	13	13	13	13	13	10	10	10	4	4	4	4	4	4	5	5	5
K* (-)	0.27	0.11	?	0.28	0.24	?	0.22	0.19	?	0.28	0.23	?	0.34	0.25	?	?	0.18	?	?	0.18	?	0.38	0.15	?
δ (cm)	-	7.1	≈18	0.5	-	6.5	12.5	-	6.5	-	-	4.8	(25)	-	?	?	-	0.3 1.5	?	-	2.3 3.8	-	-	?
ε (%)	≈2.0	≈0.3	≈0.3	≈0.4	≈0.3	0.2÷0.6	≈0.4	≈0.3	?	≈1.2	≈1.0	0.75	0.85	0.75	1.0	?	0.6 2.0	0.1 0.9	?	0.6 2.0	0.1 0.9	3.7	1.2	0.2
α (kN/m)	17.5	6.6	2.9÷6.9	7.6	6.5	2.5÷7.0	7.8	6.7	?	11.3	9.3	3.8÷8.8	14.0	12.3	16.5	?	5.4 13.5	2.5 7.0	?	5.4 13.5	2.5 7.0	23.0	6.4	2.2
FS1	0.9 ÷ 2.3			0.9 ÷ 3.2			?			1.05 ÷ 2.4			0.75			2.16; 1.93			2.16; 1.93			2.9		
FS2	2.7			1.2			1.16			1.21			1.14			?			?			3.6		
FS3	2.5 ÷ 6.1			1.2			?			1.28 ÷ 2.9			0.85			?			?			10.9		
FS4	11.3 ÷ 27.0			11.5 ÷ 32.0			?			9.10 ÷ 21.0			3.0			32.0; 11.4			32.0; 11.4			27.2		
FS5	4.5 ÷ 10.8			4.2 ÷ 11.6			?			2.40 ÷ 5.6			(2.4)			11.6; 4.1			11.6; 4.1			13.6		

Reported data: height of slope or wall H; slope angle β; uniform (or equivalent) surcharge q; unit weight of fill soil γ; global Factor of Safety FSg; angle of internal friction Φ' and cohesion c' of fill soil; pore pressure parameter Ru; peak and allowable tensile strength of geogrids used, α_f and α_a; number of geogrid layers N; coefficient of lateral soil pressure K* ; outward movement of top of slope or wall face δ; maximum tensile strain and force along geogrids, ε and α.

Formulas used for the conditions D and C:

- $\Phi' = \Phi'_M$ / FSg
- $K^* = f(\Phi', \beta, Ru)$ from design charts for slopes (Jewell et al., 1984)
- $K^* = \tan^2(45 - \Phi'/2)$ for walls
- required total tensile force: $T = 1/2 \cdot K^* \cdot \gamma \cdot (H + q/\gamma)^2$
- $\alpha = T/N$
- $\varepsilon = f(\alpha)$ measured from stress strain curve of geogrid.
- ε_M = from measurements
- α_M = measured or from stress-strain curve of the geogrid as a function of ε_M.

Partial Factors of Safety:

- FS1 = α_c / α_M
- FS2 = α_D / α_c
- FS3 = α_D / α_M
- FS4 = α_f / α_M
- FS5 = α_a / α_M

loped against the face, an hypothesis can be done based on the results of Lithonia wall measurements (Berg et al 1986): as shown in Fig. 5, it seems that the actual lateral pressure diagram is parallel to the Rankine theoretical line; this fact suggests that the lateral constriction due to interlocking, typical of geogrids, makes the soil to have a fictitious cohesion $c^{\wedge}$, which shifts the lateral pressure diagram downward. So the thrustes against the wall, and therefore the forces in the geogrids, are lower than predicted with usual Rankine theory.

With refererence to the mechanism of movement of the wall face, a hypothesis can be done, based on the results of some field tests where an outward rotation around the toe was noted (Berg et al 1986; Bathurst et al 1987). Then if we suppose that the toe can also have a translation, we have the situation shown in Fig. 6. If the geogrids are equally spaced, we can write:

$F_1 = K \cdot \gamma \cdot h_1 \cdot \delta h \quad \ldots \quad F_4 = K \cdot \gamma \cdot h_4 \cdot \delta h$

and: $\varepsilon = f(K \cdot \gamma \cdot h \cdot \delta h) = f(\gamma h)$.

Called δx the total movement of the face, then δx is the sum of the elongation of the geogrids due to tensile forces, $\varepsilon \cdot L$, and of the pull-out movement S. We can write that S is a function of the difference between the tensile force and the pull-out resistance:

$S = f(K \cdot \gamma \cdot h \cdot \delta h - 2 \cdot f_p \cdot \tan \Phi' \cdot \gamma \cdot h) = g(\gamma h)$

where f_p is the pull-out coefficient ($f_p \approx 0.7 \div 1.0$). Then we can suppose that the diagrams $S = g(\gamma h)$ and $\varepsilon = f(\gamma h)$ have the patterns shown in Fig. 7. Therefore the two components $\varepsilon \cdot L$ and S combine to form δx as shown in Fig. 8a: this is the mechanism of movement of a wall which toe can translate.

If, instead, the toe cannot translate, then we have to add a third element W to obtain the diagram of δx, as shown in Fig. 8b. W is the variation of movement of the wall due to bending stiffness of the face: it gives a negative contribution at toe and a positive contribution at top, the latter only if the vicinity of surcharge can locally increment the curvature. This mechanism says also that near the toe the wall face supports a part of the thrust: so if the surcharge is high, the lower geogrid layers have less tension than the upper ones.

With reference to the σ_v distribution, we can compare the results of Tucson and Kingston walls: as shown in Fig. 9, there were different results from similar walls; so the matter has to be furthermore investigated.

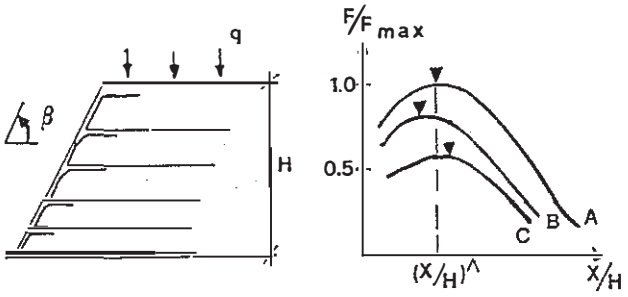

Fig. 1 - Tensile forces in a slope. A = medium-low layers; B = lower layers; C = upper layers.

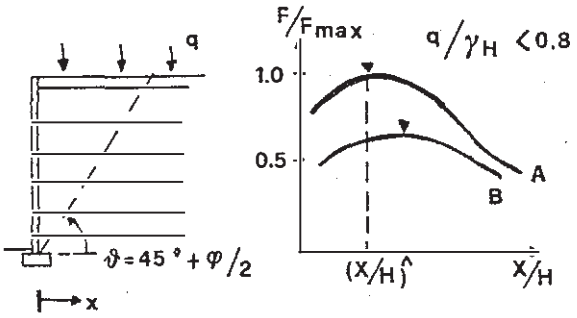

Fig. 2 - Tensile forces in a wall. A = lower layers; B = upper layers.

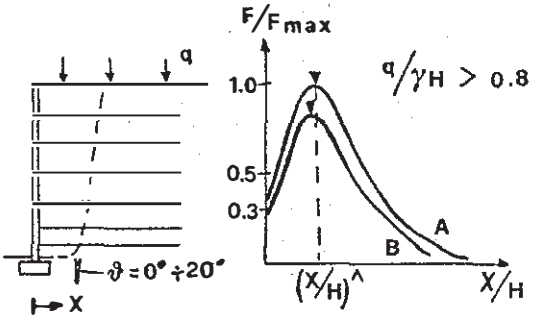

Fig. 3 - Tensile forces in a wall. A = upper layers; B = lower layers.

6 CONCLUSIONS AND PROPOSALS

Some hypotheses were done in this paper to explain the field results but, since the comparable data are too few to draw a definitive evaluation or to have a statistic confirmation, it would be useful to run firstly many small scale tests in order to investigate each of the unclear matters; then other full scale tests will give confirmation of the obtained results, allowing to control that no scale effect has occurred in the small scale tests. Only at this stage, FEM models will allow to investigate in details the distribution of each parameter throghout the reinforced soil mass. The knowledge so gained will finally allow to issue new and more accurate design methods, specific for each category.

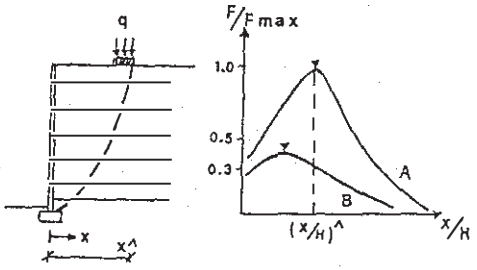

Fig. 4 - Tensile forces in a wall. A = upper layers; B = lower layers.

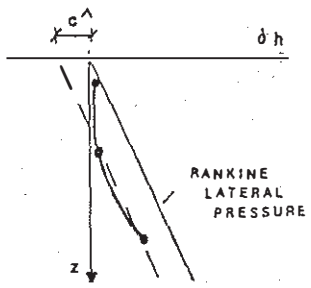

Fig. 5 - Lateral earth pressure and fictitious cohesion

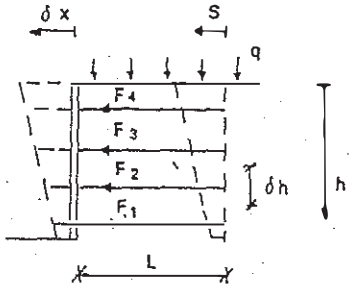

Fig. 6 - Movements of wall face.

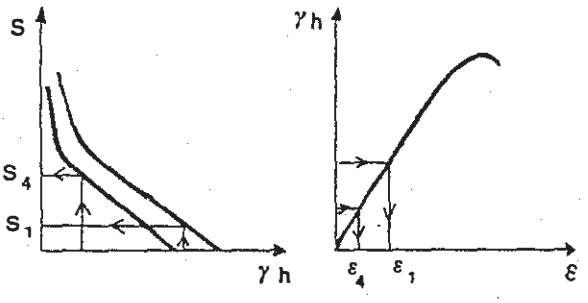

Fig. 7 - $S = g(\gamma h)$ and $\varepsilon = f(\gamma h)$.

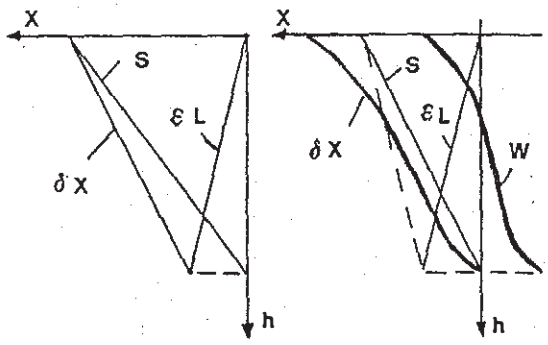

Fig. 8 - Superposition of movements with and without toe translation.

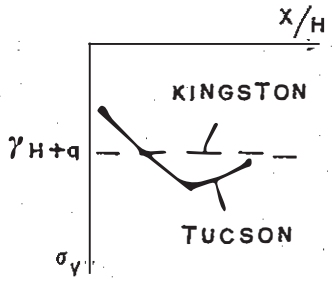

Fig. 9 - Vertical pressures at base.

REFERENCES

Bassett, R.A. et al 1986. Proceeding of Reinforced Embankment Prediction Symposium. King's College. London.

Bathurst, R.J., Wawrychuk, W.F, Jarret, P.M. 1987. Laboratory investigation of two large scale geogrid reinforced earth wall. Proc. NATO A.R.W. on Application of Polymeric Reinforcement in Soil retaining Structures. RMC. Kingston.

Berg, R.R., Bonaparte, R., Anderson, R.P., chouery, V.E., 1986. Design, construction and performance of two geogrid reinforced soil retaining walls. Proc. III Int. Conf. on Geotextiles. Vienna.

Berg, R.R., La Rochelle, P., Bonaparte, R., Tanguay, L., 1987. Gaspe Peninsula reinforced soil seawall case history. Proc. ASCE Symp. on Soil Improvement. Atlantic City.

Carroll, R.G., Richardson G.N. 1986. Geosynthetic reinforced retaining walls. Proc. III Int. Conf. on Geotextiles. Vienna.

Christopher, B.R. 1987. Geogrid reinforced soil retaining wall to widen an earth dam and support high live loads. Proc. Geosynthetics'87 conference. New orleans.

Cazzuffi, D., Pagotto, A., Rimoldi, P. 1988. Behaviour of a geogrid reinforced embankment over waste material. Proc. II Int. Conf. on Case Histories in Geotechnical Engineering. St. Louis.

Jewell, R.Q., Paine, N., Woods, R.I. 1984. Design methods for steep reinforced embankments. Proc. Symp. on Polymer Grid Reinforcement in Civil Engineering. London.

Jones, C.F.J.P. 1985. Earth reinforcement and soil structures. London: Butterworths.

Yamanuchi, T., Fukuda, N., Ikegami, M. 1986. Design and techniques of steep reinforced embankment without edge supporting. Proc. III Int. Conf. on Geotextiles. Vienna.